Int. J. Solids Structures Vol. 21, No. 12, pp. 1181–1195, 1985
Printed in Great Britain.

0020–7683/85 $3.00 + .00

LARGE DEFORMATIONS OF IN-PLANE BEAM

M. SAJE and S. SRPČIČ
Edvard Kardelj University in Ljubljana, Faculty for Architecture, Civil Engineering and Survey, Jamova 2, 61000 Ljubljana, Yugoslavia

(*Received* 28 *May* 1985)

Abstract—A theory of large deformations of straight slender in-plane beam is presented, based on the assumption of uniaxiality of the strain tensor. The integration of the compatibility conditions gives the parabolic variation of the axial component of the strain tensor over the cross-section of the beam. The integration of the kinematic equations gives linear variation of the displacement components over the cross-section. The equilibrium equations are written on a deformed configuration and numerically solved for linear elastic cantilever, subjected to concentrated or distributed conservative and nonconservative loads.

1. INTRODUCTION

The majority of theories of large deformations of slender beams is based on the Bernoulli–Euler hypothesis that the cross-sections which are perpendicular to the centroid locus before bending remain plane and perpendicular to the deformed locus and suffer no strains in their planes[1, 2]. This hypothesis is equivalent to assuming a linear variation of displacements over the cross-section.

The present paper presents an alternative theory based on the hypothesis that the strain tensor is uniaxial. By using the hypothesis in the compatibility conditions, these may be analytically integrated, giving the parabolic variation of the axial component of the strain tensor over the cross-section. When the parabolic variation of the axial strain is employed, the integration of the kinematic equations gives linear variation of the displacements over the cross-section. This shows that the present hypothesis leads to the Bernoulli–Euler beam.

The associated equilibrium equations are given in Section 3. These equations have been numerically solved for a linear elastic material and a cantilever beam subjected to conservative or nonconservative loads. The numerical procedure and numerical examples are presented in Sections 4 and 5.

2. DISPLACEMENTS DETERMINATION

Let the locus of the centroid of the cross-section of the undeformed beam be a straight line, and let it coincide with z^1 axis of the Cartesian coordinate system (z^1, z^2, z^3) with $\mathbf{e}_1$, $\mathbf{e}_2$, $\mathbf{e}_3$ as the unit base vectors. Let the cross-section $S^0_{(1)}$ of the beam in the coordinate plane z^1 = const be symmetric with respect to the coordinate plane $z^2 = 0$. The Lagrangian description is used with the initial undeformed configuration taken as reference. A material particle is identified by material coordinates $x^1 \equiv x$, $x^2 \equiv y$ and $x^3 \equiv z$, which coincide with the Cartesian coordinates z^1, z^2, z^3 in the reference configuration. The material base vectors in the reference and in the current deformed configuration are denoted by $\mathbf{g}_1$, $\mathbf{g}_2$, $\mathbf{g}_3$ and $\mathbf{G}_1$, $\mathbf{G}_2$, $\mathbf{G}_3$ (Fig. 1).

We now introduce the assumption that the components γ_{12}, γ_{13}, γ_{22}, γ_{23} and γ_{33} of the Lagrangian strain tensor may be neglected in comparison with the component γ_{11}. Hence

$$\gamma_{11} = \gamma_{11}(x, z), \tag{1}$$

$$\gamma_{12} = \gamma_{13} = \gamma_{22} = \gamma_{23} = \gamma_{33} = 0. \tag{2}$$

The covariant and contravariant components of the deformed metric tensor, G_{ij} and

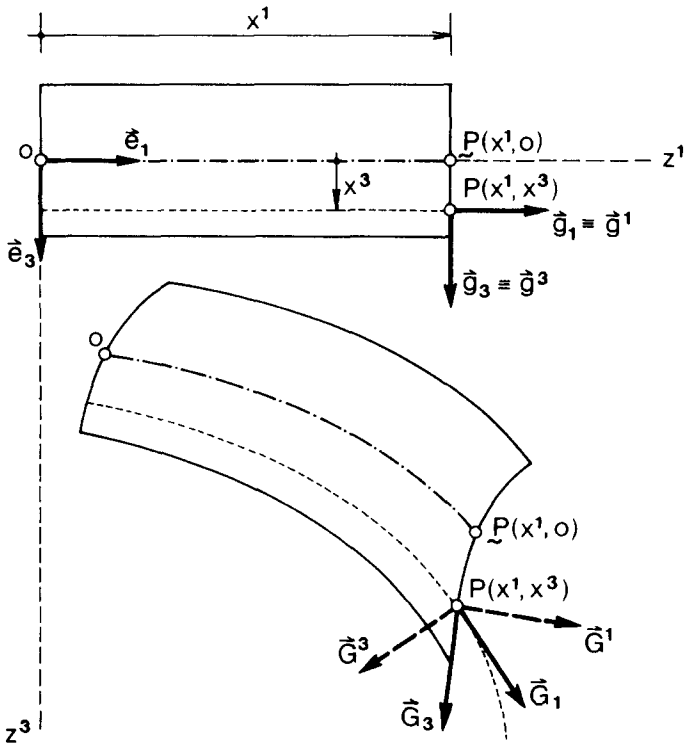

Fig. 1. Beam element. Initial and deformed configurations. Coordinate systems and base vectors.

G^{ij}, are determined by the equations

$$G_{ij} = g_{ij} + 2\gamma_{ij}, \tag{3}$$

$$G^{ij} = G_{ij}^{-1}, \tag{4}$$

where g_{ij} denotes the covariant components of the undeformed metric tensor. The application of (1) and (2) in (3) and (4) gives

$$\begin{aligned} G_{11} &= 1 + 2\gamma_{11}, \\ G_{22} &= G_{33} = 1, \\ G_{12} &= G_{13} = G_{23} = 0. \end{aligned} \tag{5}$$

and

$$\begin{aligned} G^{11} &= \frac{1}{1 + 2\gamma_{11}}, \\ G^{22} &= G^{33} = 1, \\ G^{12} &= G^{13} = G^{23} = 0. \end{aligned} \tag{6}$$

The components (1) and (2) of the strain tensor must satisfy compatibility conditions. These require vanishing of the components of the Riemann–Christoffel curvature tensor R_{ijkl} in a deformed configuration[3]:

$$\begin{aligned} R_{ijkl} = {} & \gamma_{jl,ik} - \gamma_{il,jk} - \gamma_{jk,il} + \gamma_{ik,jl} - G^{\alpha\beta}\,[(\gamma_{j\beta,k} + \gamma_{k\beta,j} - \gamma_{jk,\beta})\,(\gamma_{i\alpha,l} \\ & - \gamma_{l\alpha,i} - \gamma_{il,\alpha}) - (\gamma_{j\beta,l} + \gamma_{l\beta,j} - \gamma_{jl,\beta})\,(\gamma_{i\alpha,k} + \gamma_{k\alpha,i} - \gamma_{ik,\alpha})] = 0. \end{aligned} \tag{7}$$

(",i" designates a partial derivative with respect to material coordinate x^i.) Substituting (1), (2) and (6) into (7) yields

$$R_{3131} = \gamma_{11,33} - \frac{(\gamma_{11,3})^2}{1 + 2\gamma_{11}} = 0, \tag{8}$$

the remaining conditions being identically satisfied. Solving eqn (8) for γ_{11} gives

$$\gamma_{11}(x, z) = \frac{1}{2}\{[A(x)z + B(x)]^2 - 1\} \tag{9}$$

where the particular form of the integration functions $A(x)$ and $B(x)$ depends on actual load, geometry, material properties and boundary conditions. Equation (9) shows that the strain component γ_{11} may vary over the cross-section quadratically with respect to z.

The contravariant components u^1 and u^3 of the displacement vector $\mathbf{u}$ of an arbitrary material particle

$$\mathbf{u} = u^1\mathbf{g}_1 + u^3\mathbf{g}_3, \tag{10}$$

and its covariant components u_1 and u_3 are related to the components of the strain tensor by the kinematic relations

$$\gamma_{ij} = \frac{1}{2}(u_{i,j} + u_{j,i} + u_{k,i}\,u^k_{,j}). \tag{11}$$

Employing eqns (2) and (9) and the fact that $u_1 = u^1$ and $u_3 = u^3$, in eqn (11), after multiplying by 2 gives

$$2\gamma_{11} = 2u^1_{,1} + (u^1_{,1})^2 + (u^3_{,1})^2 = (B^2 - 1) + 2ABz + A^2z^2, \tag{12}$$

$$2\gamma_{13} = u^1_{,3} + u^3_{,1} + u^1_{,1}u^1_{,3} + u^3_{,1}u^3_{,3} = 0, \tag{13}$$

$$2\gamma_{33} = 2u^3_{,3} + (u^1_{,3})^2 + (u^3_{,3})^2 = 0, \tag{14}$$

$$\gamma_{12} = \gamma_{13} = \gamma_{23} \equiv 0. \tag{15}$$

The eqns (12)–(14) constitute a system of three nonlinear partial-differential equations for the two displacement components $u^1(x, z)$ and $u^3(x, z)$. The existence of single-valued solution of the system has been assured by satisfying the compatibility eqns (7) and (8).

Equations (12)–(14) may be solved explicitly by the substitution in a form of polynomial:

$$u^1(x, z) = \alpha_0(x) + \alpha_1(x)z + \alpha_2(x)z^2 + \cdots + \alpha_m(x)z^m, \tag{16}$$

$$u^3(x, z) = \beta_0(x) + \beta_1(x)z + \beta_2(x)z^2 + \cdots + \beta_n(x)z^n. \tag{17}$$

From eqns (14), (16) and (17) we obtain the system of algebraic equations

(14): $z^0 \ldots 2\beta_1 + \alpha_1^2 + \beta_1^2 = 0,$ (18)

$z^1 \ldots 4\beta_2 + 4\alpha_1\alpha_2 + 4\beta_1\beta_2 = 0,$ (19)

$$\vdots$$

$$z^{2(p-1)} \ldots \begin{cases} m^2\alpha_m^2 + n^2\beta_n^2 = 0 & \text{for } p = m = n \geqslant 2, \\ m^2\alpha_m^2 = 0 & \text{for } p = m \geqslant n \text{ and } m \geqslant 2, \\ n^2\beta_n^2 = 0 & \text{for } p = n \geqslant m \text{ and } n \geqslant 2. \end{cases} \tag{20}$$

Equation (20) requires

$$\alpha_m = 0, \qquad \beta_n = 0. \tag{21}$$

Using (21) in (19) implies that $\alpha_i = 0$ and $\beta_i = 0$ for $i \geqq 2$. Hence

$$u^1 = \alpha_0 + \alpha_1 z, \tag{22}$$

$$u^3 = \beta_0 + \beta_1 z. \tag{23}$$

Applying (22) and (23) in (12) and (13), leads

$$\text{(12):} \quad 2\alpha_0' + \alpha_0'^2 + \beta_0'^2 = B^2 - 1, \tag{24}$$

$$2\alpha_1' + 2\alpha_0'\alpha_1' + 2\beta_0'\beta_1' = 2AB, \tag{25}$$

$$\alpha_0'^2 + \beta_0'^2 = A^2, \tag{26}$$

$$\text{(13):} \quad \alpha_1 + \beta_0' + \alpha_0'\alpha_1 + \beta_0'\beta_1 = 0, \tag{27}$$

$$\beta_1' + \alpha_1'\alpha_1 + \beta_1'\beta_1 = 0. \tag{28}$$

(The prime ′ denotes differentiation with respect to x.) The nonlinear differential equations (24)–(28) and algebraic equation (18) constitute a system of six equations for four unknown functions α_0, α_1, β_0 and β_1. This system may be solved explicitly by first solving (18) and (26) for α_1 and β_1, and then integrating (25) and (27) for α_0 and β_0. The integration gives

$$\alpha_0(x) = u^1(x_0, 0) + \int_{x_0}^{x} [B(\xi) \cos \omega(\xi) - 1]\, d\xi, \tag{29}$$

$$\beta_0(x) = u^3(x_0, 0) - \int_{x_0}^{x} B(\xi) \sin \omega(\xi)\, d\xi, \tag{30}$$

$$\alpha_1(x) = \sin \omega(x), \tag{31}$$

$$\beta_1(x) = \cos \omega(x) - 1, \tag{32}$$

where $u^1(x_0, 0)$ and $u^3(x_0, 0)$ are the displacement components, evaluated at the reference material particle $(x_0, 0)$, and the notation $\omega(x)$ has been introduced:

$$\omega(x) = \int_{x_0}^{x} A(\xi)\, d\xi + \arcsin \left(\frac{\partial u^1}{\partial z} \right)_{x = x_0}, \tag{33}$$

where $(\partial u^1/\partial z)_{x=x_0}$ designates the displacement derivative at the reference particle $(x_0, 0)$.

The base vectors of the deformed configuration are determined from the displacements by the relation

$$\mathbf{G}_i = (\delta_i^m + u_{,i}^m)\mathbf{g}_m. \tag{34}$$

(δ_i^m denotes the Kronecker symbol.) Combining eqns (22)–(23), (29)–(33) and (34) gives the covariant base vectors

$$\begin{aligned} \mathbf{G}_1 &= (\omega' z + B)(\mathbf{g}_1 \cos \omega - \mathbf{g}_3 \sin \omega), \\ \mathbf{G}_2 &= \mathbf{g}_2 \\ \mathbf{G}_3 &= \mathbf{g}_1 \sin \omega + \mathbf{g}_3 \cos \omega. \end{aligned} \tag{35}$$

The associated contravariant base vectors are

$$\mathbf{G}^1 = \frac{1}{\omega' z + B}(\mathbf{g}_1 \cos\omega - \mathbf{g}_3 \sin\omega),$$
$$\mathbf{G}^2 = \mathbf{g}_2 \tag{36}$$
$$\mathbf{G}^3 = \mathbf{g}_1 \sin\omega + \mathbf{g}_3 \cos\omega.$$

The functions $A(x)$ and $B(x)$ have physical significance. A physical meaning of A is found by comparing deformed and undeformed directions of centroidal axis. It is then established that A is the derivative of the centroid axis rotation φ with respect to x:

$$A(x) = \varphi'(x). \tag{37}$$

Hence

$$\varphi(x) = \omega(x). \tag{38}$$

Physical character of B is shown by employing eqn (5) in the expression for unit extension D_1:

$$D_1(x, z) = \sqrt{G_{11}} - 1 = \varphi' z + B - 1. \tag{39}$$

Introducing notation ϵ for unit extension of centroid axis

$$\epsilon(x) = D_1(z = 0) = B - 1 \tag{40}$$

gives

$$B(x) = 1 + \epsilon(x). \tag{41}$$

The results obtained in this section indicate that, as a consequence of assumptions (1) and (2), the deformation of the beam is described by the two functions $\varphi(x)$ and $\epsilon(x)$, the rotation and the unit extension of the centroid axis of the beam; that the displacement components u^1 and u^3 vary linearly over the cross-section; initially undeformed planar cross-section remains planar and perpendicular to the locus of centroids after deformation; its shape and its area are preserved ($S_{(1)} = S^0_{(1)}$). The assumptions (1) and (2) lead therefore to the Bernoulli–Euler hypothesis.

3. EQUILIBRIUM EQUATIONS

Within the framework of static analysis the equilibrium equations for a beam are given by the differential equations

$$\frac{\mathrm{d}\mathbf{N}}{\mathrm{d}x} + \mathcal{P} = \mathbf{0}, \tag{42}$$

$$\frac{\mathrm{d}\mathbf{M}}{\mathrm{d}x} + \mathbf{G}_1 \times \mathbf{N} + \mathcal{M} = \mathbf{0}. \tag{43}$$

$\mathbf{N}$ and $\mathbf{M}$ are the stress resultants vectors at the cross-section of the beam, given by the expressions

$$\mathbf{N} = N\frac{\mathbf{G}^1}{\sqrt{G^{11}}} + Q\frac{\mathbf{G}_3}{\sqrt{G_{33}}}, \tag{44}$$

$$\mathbf{M} = M\frac{\mathbf{G}_2}{\sqrt{G_{22}}}, \tag{45}$$

where N, Q and M denote axial force, shear force and bending moment of the cross-section. $\mathcal{P}$ and $\mathcal{M}$ are distributed external force and moment per unit undeformed length

$$\mathcal{P} = \mathcal{P}_0^1 \mathbf{g}_1 + \mathcal{P}_0^3 \mathbf{g}_3, \tag{46}$$

$$\mathcal{M} = \mathcal{M}_0 \mathbf{g}_2. \tag{47}$$

$\mathbf{G}_1$ denotes the base vector $\mathbf{G}_1$ at $z = 0$:

$$\mathbf{G}_1 = \mathbf{G}_1(z = 0) = (1 + \epsilon)(\mathbf{g}_1 \cos \varphi - \mathbf{g}_3 \sin \varphi). \tag{48}$$

Substituting eqns (44) and (45) into (42) and (43), and employing (35), (36), (38) and (41) yields

$$N = R^1 \cos \varphi - R^3 \sin \varphi \tag{49}$$

$$Q = R^1 \sin \varphi + R^3 \cos \varphi, \tag{50}$$

$$\frac{dM}{dx} - Q(1 + \epsilon) + \mathcal{M}_0 = 0. \tag{51}$$

R^1 and R^3 are the components of the negative external load resultants at x with respect to a reference coordinate x_0:

$$R^1 = [N \cos \varphi + Q \sin \varphi]_{x=x_0} - \int_{x_0}^{x} \mathcal{P}_0^1(\xi)\, d\xi, \tag{52}$$

$$R^3 = [-N \sin \varphi + Q \cos \varphi]_{x=x_0} - \int_{x_0}^{x} \mathcal{P}_0^3(\xi)\, d\xi. \tag{53}$$

The constitutive law for material is assumed to be given by a linear elastic relation between the longitudinal "true" stress component $\sigma_{(1)}$ and the associated unit extension D_1

$$\sigma_{(1)} = LD_1 \tag{54}$$

where L is elastic modulus of material. Using relations (54), (39) and (41), N and M take the form

$$N = \int_{S_{(1)}} \sigma_{(1)}\, dS = LS^0_{(1)}\epsilon, \tag{55}$$

$$M = \int_{S_{(1)}} z\, \sigma_{(1)}\, dS = LI_y^0 \frac{d\varphi}{dx}, \tag{56}$$

where I_y^0 is the moment of inertia of the cross-section with respect to the y axis. Elimination of N, Q, M and ϵ from (51) by employing eqns (49), (50), (51), (55) and (56), gives the differential equation for φ

$$LI_y^0 \frac{d^2\varphi}{dx^2} - (R^1 \sin\varphi + R^3 \cos\varphi)\left[1 + \frac{1}{LS^0_{(1)}}(R^1 \cos\varphi - R^3 \sin\varphi)\right] + \mathcal{M}_0 = 0. \tag{57}$$

Introducing notation $u = u^1(z = 0)$ and $w = u^3(z = 0)$ for the displacement components along the centroid axis, and using eqns (22)–(23) and (29)–(33), yields

$$u(x) = u(x_0) + \int_{x_0}^{x} [(1 + \epsilon) \cos \varphi - 1]\, d\xi, \tag{58}$$

$$w(x) = w(x_0) - \int_{x_0}^{x} (1 + \epsilon) \sin \varphi\, d\xi. \tag{59}$$

Equations (49)–(51), (55), (56), (58) and (59) constitute a system of seven equations for seven unknown functions N, Q, M, φ, ϵ, u and w. These equations can be solved uniquely for the prescribed geometric characteristics, material parameter, boundary conditions and external loads.

4. METHOD OF SOLUTION

We consider a cantilever beam of undeformed length, l, subject to concentrated or distributed conservative and nonconservative loads, whose equilibrium is governed by the differential equation (57). This equation is solved here by the finite difference method. The integration region $x \in [0, l]$ is divided into n equal subregions by $n + 1$ equally spaced nodes 1, 2, 3, . . . , $n + 1$ with the coordinates $x_1 = 0$, $x_2 = h$, $x_3 = 2h$, . . . , $x_{n+1} = l$, then the differential equation is replaced by the difference equation in each node. By utilizing the lowest-order difference approximation for the second derivative, the differential equation (57), written for a typical node "i", takes the form

$$\frac{LI_y^0}{h^2}(\varphi_{i+1} - 2\varphi_i + \varphi_{i-1}) - (R_i^1 \sin\varphi_i + R_i^3 \cos\varphi_i) \times \left[1 + \frac{1}{LS_{(1)}^0}(R_i^1 \cos\varphi_i - R_i^3 \sin\varphi_i)\right] + \mathcal{M}_{0i} = 0, \quad (60)$$

where $h = l/n$, and φ_i, R_i^1, R_i^3 and $\mathcal{M}_{0i}$ are the values of φ, R^1, R^3 and $\mathcal{M}_0$ at the node i. By writing eqn (60) at $n + 1$ nodes, and taking into account appropriate static and kinematic boundary conditions at $x = 0$ and $x = l$, a system of nonlinear transcendental equations for nodal values φ_i is obtained. This system has been solved iteratively, employing the Newton method.

Special case. There is a special case when the procedure gives the system of nonlinear equations, the solution of which requires no iteration and is given by simple recurrence formula. It is the case when the cantilever is subject, at its free end, only to the tangential (T_1) and normal (P_1) forces and to the moment (Z_1), and to the distributed moment ($\mathcal{M}_0$) acting along the axis of the beam. Let us take a detailed look at the case.

We introduce the relative rotation

$$\phi(x) = \varphi(x) - \varphi_1 \quad (61)$$

(φ_1 stands for rotation of the node 1), put $\mathcal{P}_0^1 = \mathcal{P}_0^3 = 0$ and employ (61), (52) and (53) in the eqn (57) and thus get

$$LI_y^0 \frac{d^2\phi}{dx^2} + (T_1 \sin\phi + P_1 \cos\phi)\left[1 + \frac{1}{LS_{(1)}^0}(-T_1 \cos\phi + P_1 \sin\phi)\right] + \mathcal{M}_0 = 0. \quad (62)$$

When replaced by their difference equations in node 1, the eqn (62) and its boundary condition

$$M(x_1) = -Z_1 = LI_y^0 \left(\frac{d\phi}{dx}\right)_{x=x_1} \quad (63)$$

give two equations for three nodal values: ϕ_0 (at the auxiliary node at $x = -h$), ϕ_1 and ϕ_2. Because ϕ_1 is zero by the definition (61), the two equations can be solved for ϕ_0 and ϕ_2, obtaining

$$\phi_0 = \frac{h}{LI_y^0} Z_1 - \frac{h^2}{2LI_y^0} P_1 \left(1 - \frac{1}{LS_{(1)}^0} T_1\right) - \frac{h^2}{2LI_y^0} \mathcal{M}_{01}, \quad (64)$$

$$\phi_1 = 0, \quad (65)$$

$$\phi_2 = -\frac{h}{LI_y^0} Z_1 - \frac{h^2}{2LI_y^0} P_1 \left(1 - \frac{1}{LS_{(1)}^0} T_1\right) - \frac{h^2}{2LI_y^0} \mathcal{M}_{01}. \quad (66)$$

Application of the above equations in the difference form of eqn (62) gives the recurrence formula from which the remaining relative nodal rotations are evaluated:

$$\phi_{i+1} = 2\phi_i - \phi_{i-1} - \frac{h^2}{LI_y^0}(T_1 \sin\phi_i + P_1 \cos\phi_i) \times \left[1 + \frac{1}{LS_{(1)}^0}(-T_1 \cos\phi_i + P_1 \sin\phi_i)\right] - \frac{h^2}{LI_y^0}\mathcal{M}_{0i}, \quad i = 2, 3, \ldots, n. \tag{67}$$

When boundary condition at the clamped end, $\varphi_{n+1} = 0$, is taken into account and eqn (61) employed, nodal rotations φ_i are obtained.

In terms of these values the nodal values of axial force, shear force, bending moment, unit extension of centroid axis and displacements are found by applying eqns (49), (50), (56), (55), (58) and (59). The trapezoidal formula has been used for the integration of the integrals (58) and (59).

5. NUMERICAL EXAMPLES

Example 1: *a cantilever subjected at its free end to the moment* (Z_1)

We consider a cantilever of length l subjected to the moment Z_1 at its free end, $x = 0$, and clamped at $x = l$. Employing $R^1 = 0$, $R^3 = 0$ and $\mathcal{M}_0 = 0$ in eqn (57), integrating and taking into account the boundary conditions $\varphi'(0) = -Z_1/LI_y^0$ and

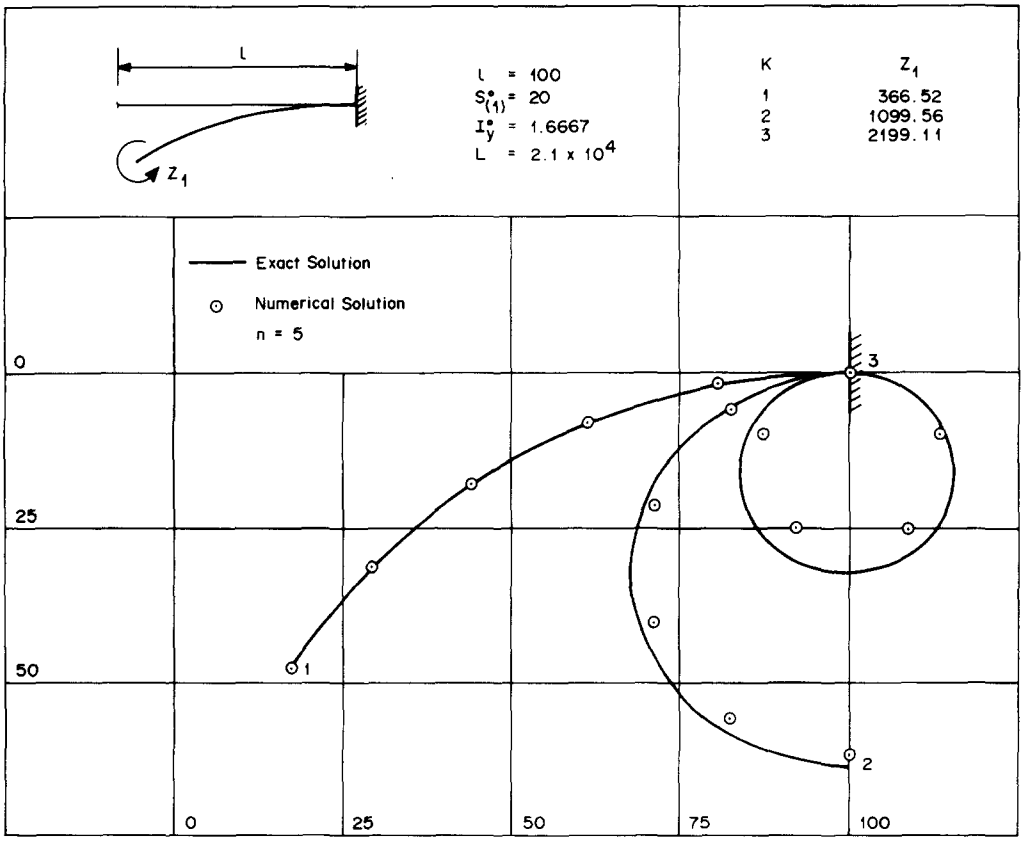

Fig. 2. Cantilever subjected at its free end to the moment (Z_1). Deformed shapes.

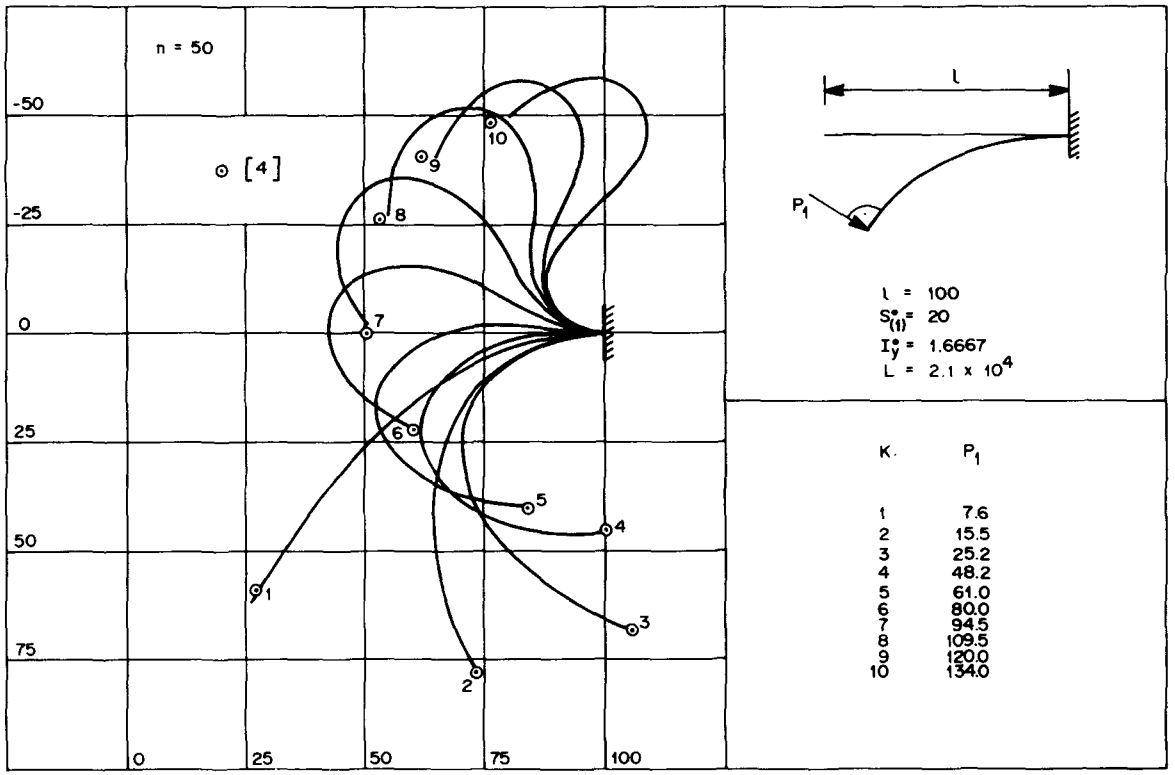

Fig. 3. Cantilever subjected at its free end to normal force (P_1). Deformed shapes.

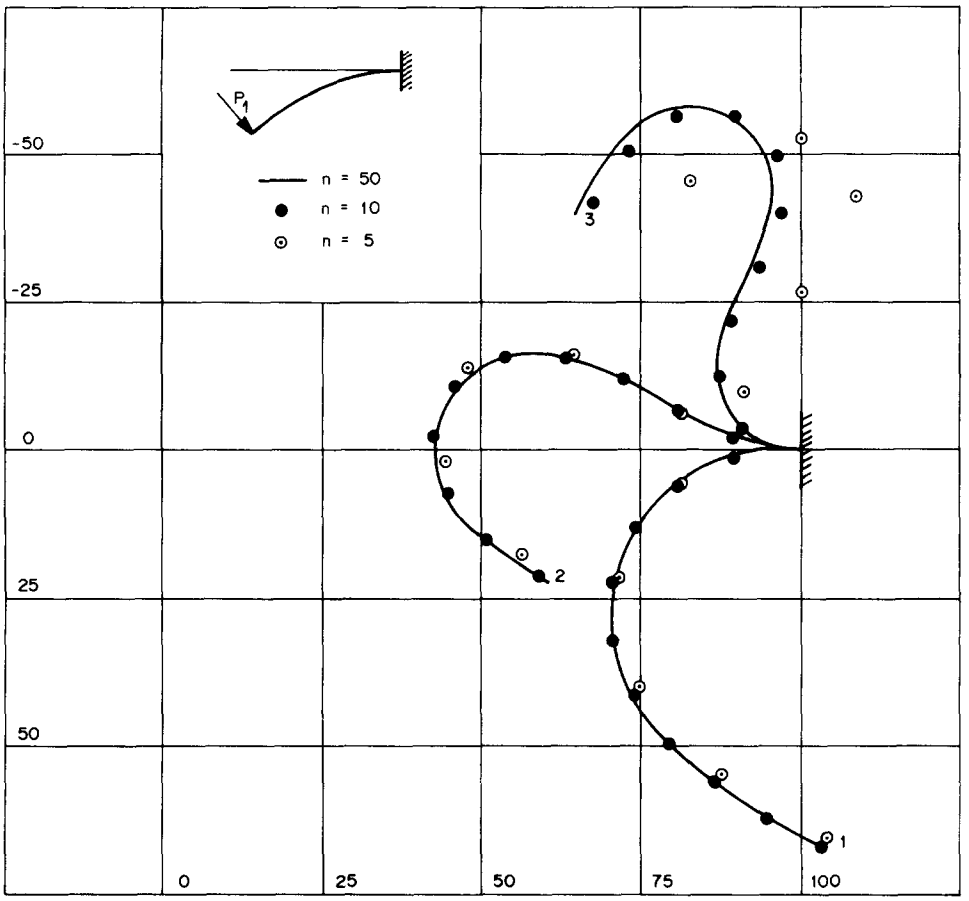

Fig. 4. Cantilever subjected at its free end to normal force (P_1). Effect of subdivision number n on deformed shape for $P_1 = 25.2$ (curve 1), $P_1 = 80.0$ (curve 2) and $P_1 = 120.0$ (curve 3).

$\varphi(l) = 0$, gives

$$\varphi(x) = \varphi_1 \left(1 - \frac{l}{x}\right), \tag{68}$$

$$\varphi_1 = \frac{Z_1 l}{L I_y^0}. \tag{69}$$

Substituting eqn (68) into (58) and (59), integrating and using the boundary conditions $u(l) = 0$ and $w(l) = 0$, yields

$$u(x) = \frac{l}{\varphi_1}\left\{-\sin\left[\varphi_1\left(1 - \frac{x}{l}\right)\right] + \varphi_1\left(1 - \frac{x}{l}\right)\right\}, \tag{70}$$

$$w(x) = \frac{l}{\varphi_1}\left\{1 - \cos\left[\varphi_1\left(1 - \frac{x}{l}\right)\right]\right\}. \tag{71}$$

These equations show that the exact deformed shape of the cantilever is a part of a circle with the curvature κ

$$\kappa = \frac{Z_1}{L I_y^0}. \tag{72}$$

Figure 2 shows the deformed shapes for various loading stages, obtained by applying the exact solution, eqns (70) and (71) (solid lines). They are compared to the shapes given by the numerical procedure defined by eqns (64)–(67) with $n = 5$. Considering that $n = 5$ is a coarse subdivision, the discrepancies are very small. When taking $n = 20$, the obtained deformed shapes are indistinguishable from the curves given by the exact solution.

Example 2: *a cantilever subjected at its free end to normal force* (P_1)

Figure 3 shows the deformed shapes of the cantilever subjected at its free end to the force P_1, the direction of which remains perpendicular to the centroid axis throughout the deformation. The shapes have been obtained by applying eqns (64)–(67) with $n = 50$. They are displayed up to the force value $P_1 = 134.0$ when, as shown in [4], the dynamic instability takes place. The deformed cantilever shapes have been compared to the closed-form solution of Lau[5], expressed in the form of elliptic integrals and to the limited results of Baumeister and Sebrosky[6] given in a graphical form as design charts. Both references assume inextensibility of the cantilever. A complete agreement has been found between the exact solutions [5] and [6] and the present solution. This also shows that the extensibility of the cantilever plays no role in a deformation of the cantilever under consideration. The deformed shapes have also been

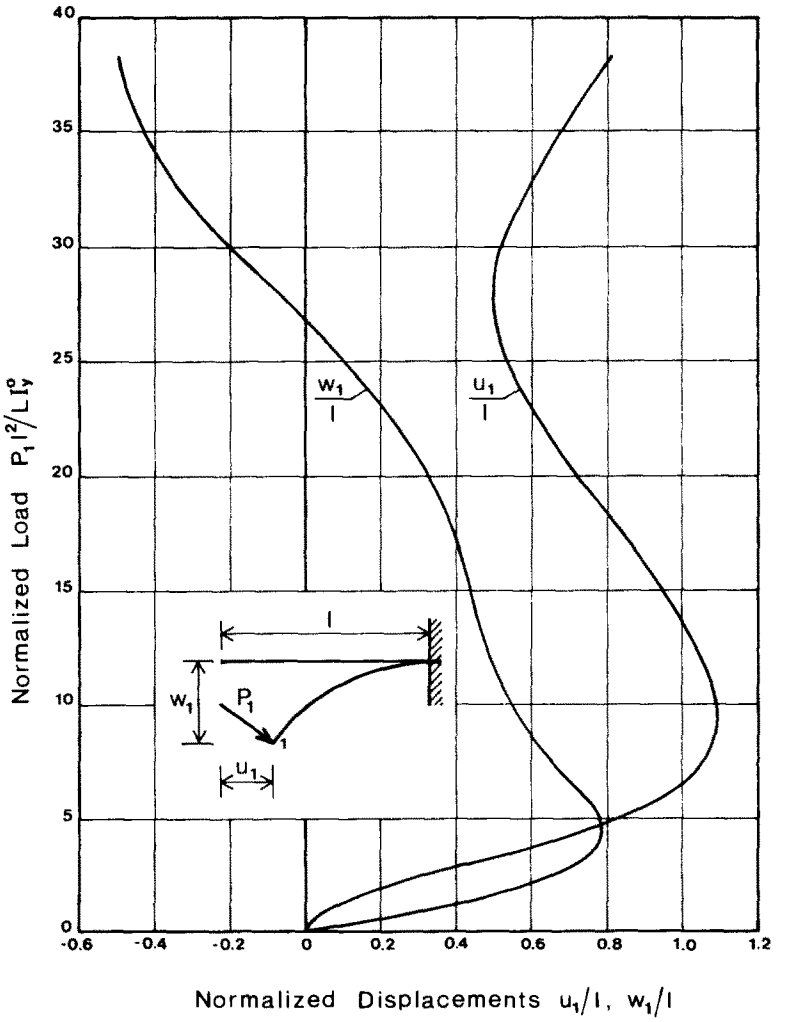

Fig. 5. Cantilever subjected at its free end to normal force (P_1). Normalized load, P_1l^2/LI_y^0, vs normalized horizonal and vertical free-end displacements, u_1/l and w_1/l.

compared to the finite element results of Argyris and Symeonidis[4]. They used 10 finite elements. The comparison is shown in Fig. 3. There is a rather good agreement between the two solutions.

Figure 4 displays the effect of the subdivision number, n, on the accuracy of the present method. The deformed shapes obtained with $n = 50$ for the forces $P_1 = 25.2$, 80.0 and 120.0, are drawn in the figure and compared to the shapes calculated by employing $n = 5$ (in the figure marked by circles) and $n = 10$ (marked by full circles). Considering that the solution with $n = 50$ represents the accurate solution, the inaccuracies obtained with relatively coarse subdivisions $n = 5$ and $n = 10$, for the curves 1 and 2, are very small. The discrepancies are however substantial for $n = 5$ and $P_1 = 120.0$, as illustrated by the figure.

Figure 5 shows normalized horizontal and vertical displacements, u_1/l and w_1/l, of the free end of the cantilever, as a function of the normalized load, $P_1 l^2/LI_y^0$.

Example 3: *a cantilever subjected to uniformly distributed normal force* (q_3) *per unit undeformed length*

Figure 6 shows the deformed shapes of the cantilever subjected to the uniformly distributed force whose direction remains perpendicular to the centroid axis throughout the deformation. The shapes have been obtained by applying the difference method in

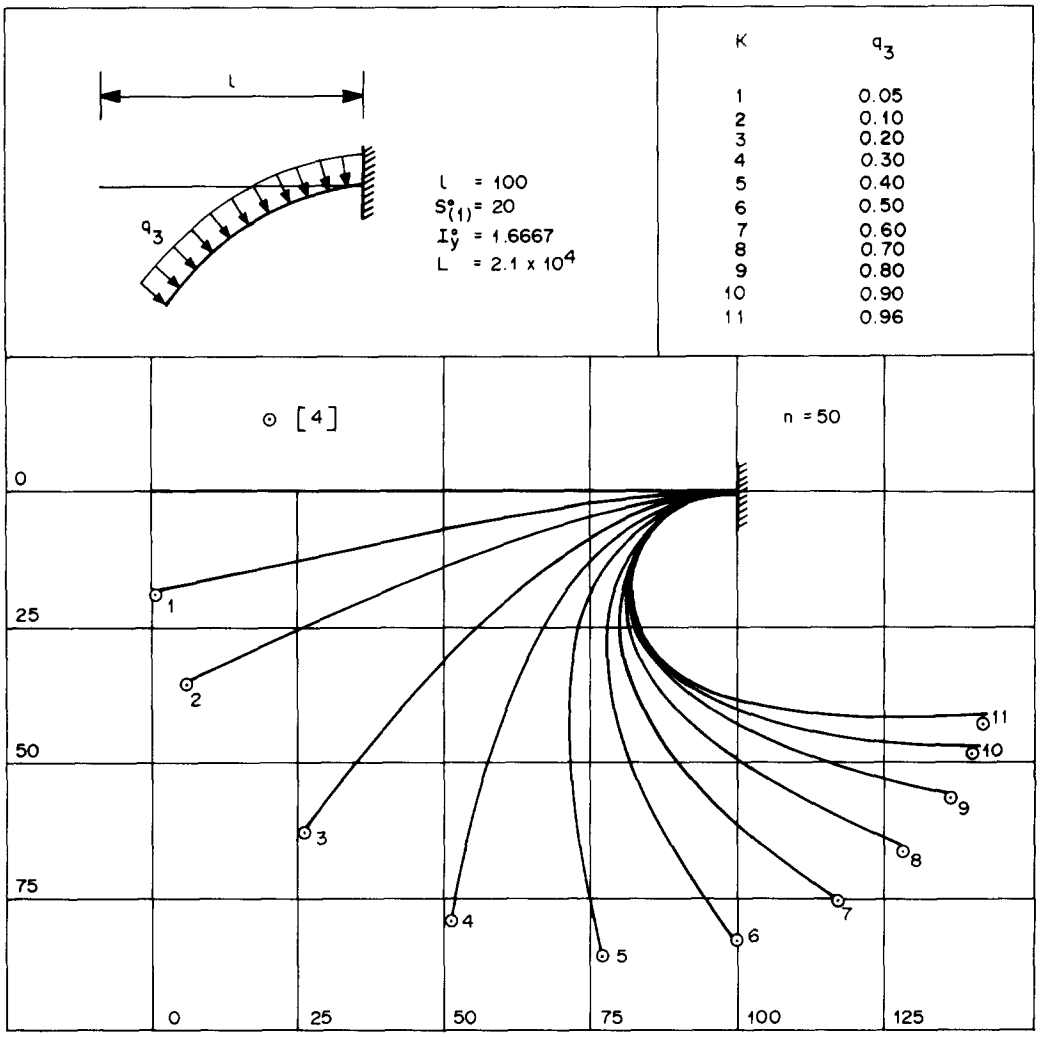

Fig. 6. Cantilever subjected to uniformly distributed normal force (q_3) per unit undeformed length. Deformed shapes.

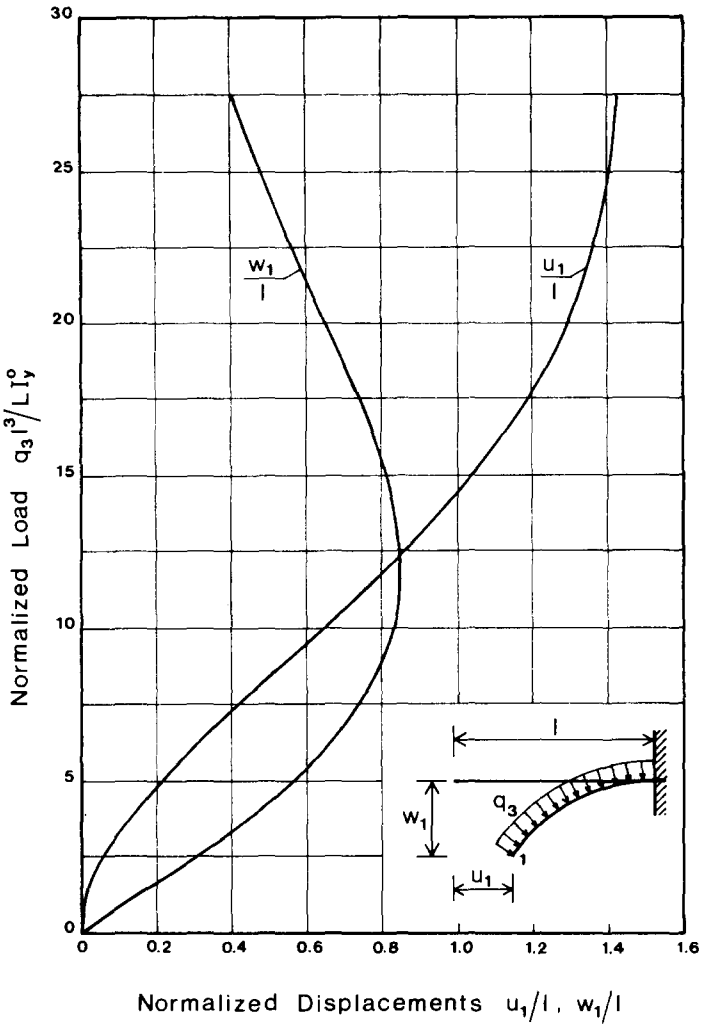

Fig. 7. Cantilever subjected to uniformly distributed normal force (q_3) per unit undeformed length. Normalized traction, q_3l^3/LI_y^0, vs normalized horizontal and vertical free-end displacements, u_1/l and w_1/l.

conjunction with the Newton iteration for the solution of eqn (60), and $n = 50$. They are shown up to the traction value $q_3 = 0.96$ when the dynamic instability takes place[4]. The deformed shapes have been compared to the closed-form solution of Mitchell[7], expressed in the form of elliptic integrals. His solution assumes inextensibility of the cantilever. A complete agreement has been found. The deformed shapes have also been compared to the finite-element results[4]. The comparison is shown in Fig. 6.

Figure 7 shows normalized horizontal and vertical displacements, u_1/l and w_1/l, of the free end as a function of the normalized traction q_3l^3/LI_y^0.

Example 4: *a cantilever subjected at its free end to horizontal force* (H_1)

Figure 8 shows the buckled shapes at various forces above the second buckling load. A small vertical force (V_1) and a moment (Z_1) at the free end were applied and later removed to initiate the deforming into the second buckling mode.

6. CONCLUSIONS

1. A theory of large deformations of straight slender in-plane beam is presented, based on the assumption of uniaxiality of the strain tensor. By using this assumption, compatibility conditions are reduced to one differential equation which is analytically

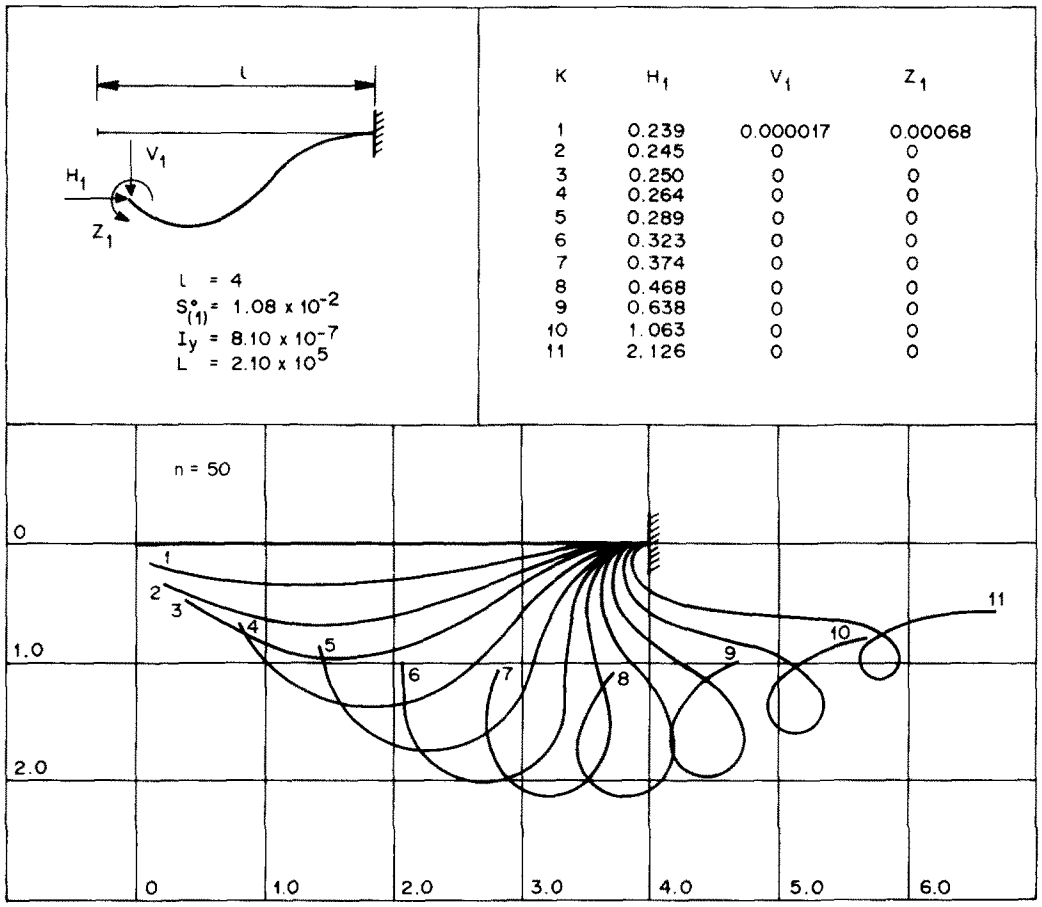

Fig. 8. Cantilever subjected at its free end to horizontal force (H_1) above the second buckling load. Deformed shapes.

integrated, giving the strain which depends on two arbitrary deformation functions of the longitudinal coordinate and varies parabolically over the cross-section. The integration of the kinematic equations gives the shape of the deformed beam as a function of two deformation functions, the unit extension ϵ, and the rotation φ of the centroid axis. The equilibrium equations are then derived which allow, within the framework of static-elastic analysis, for large strains of any magnitude.

2. The hypothesis that the strain tensor is uniaxial requires the linear variation of the displacements over the cross-section. This hypothesis is therefore equivalent to the Bernoulli–Euler hypothesis.

3. The equilibrium equations of the beam are solved by the use of the finite-difference method. The comparison between numerical and analytic solutions shows very good agreement even for coarse subdivisions. It is therefore anticipated that good solutions may be expected with the present method for problems for which analytic solutions are not available.

4. In the present theory extensibility of the beam is taken into account. The comparisons with the analytic results[5–7], which assume inextensible cantilever, show that the extensibility has no effect on the results.

5. The static analysis presented here sets no limits to the magnitude of the deformation. In an actual structure these limits may be defined by the dynamic instabilities.

Acknowledgement—This work was supported by the Research Council of Slovenia under the Contract C2-0138-792.

REFERENCES

1. A. Pflüger, *Stabilitätsprobleme der Elastostatik*. Springer-Verlag, Berlin Heidelberg (1964).
2. J. Banovec, An efficient finite element method for elastic–plastic analysis of plane frames. In *Nonlinear Finite Element Analysis in Structural Mechanics* (Edited by W. Wunderlich, E. Stein and K.-J. Bathe), pp. 385–402. Springer-Verlag, Berlin Heidelberg (1981).
3. I. S. Sokolnikoff, *Tensor Analysis*. John Wiley, New York (1964).
4. J. H. Argyris and S. Symeonidis, Nonlinear finite-element analysis of elastic systems under nonconservative loading—natural formulation, Part I: Quasistatic problems. *Comp. Meths. Appl. Mech. Eng.* **26,** 75–123 (1981).
5. J. H. Lau, Large deflections of beams with combined loads. *Proc. ASCE J. Eng. Mech. Div.* **108**(EM1), 180–185 (1982).
6. H. K. Baumeister and R. A. Sebrosky, Pushing cantilever springs to the limit. *Mach. Des.* Dec. 12, 140–143 (1974).
7. T. P. Mitchell, The nonlinear bending of thin rods. *J. Appl. Mech., Trans. ASME* **26,** 40–43 (1959).